JACS
JOURNAL OF THE AMERICAN CHEMICAL SOCIETY

ARTICLE

pubs.acs.org/JACS

Deep Penetration of a PDT Drug into Tumors by Noncovalent Drug-Gold Nanoparticle Conjugates

Yu Cheng,[§,†] Joseph D. Meyers,[§,†,‡] Ann-Marie Broome,[*,‡] Malcolm E. Kenney,[†] James P. Basilion,[*,‡] and Clemens Burda[*,†]

[†]Department of Chemistry, [‡]Departments of Biomedical Engineering and Radiology, NFCR Center for Molecular Imaging, Case Western Reserve University, Cleveland, Ohio 44106, United States

Supporting Information

ABSTRACT: Efficient drug delivery to tumors is of ever-increasing importance. Single-visit diagnosis and treatment sessions are the goal of future theranostics. In this work, a noncovalent PDT cancer drug-gold nanoparticle (Au NP) conjugate system performed a rapid drug release and deep penetration of the drug into tumors within hours. The drug delivery mechanism of the PDT drug through Au NPs into tumors by passive accumulation was investigated via fluorescence imaging, elemental analysis, and histological staining. The pharmacokinetics of the conjugates over a 7-day test period showed rapid drug excretion, as monitored via the fluorescence of the drug in urine. Moreover, the biodistribution of Au NPs in this study period indicated clearance of the NPs from the mice. This study suggests that noncovalent delivery via Au NPs provides an attractive approach for cancer drugs to penetrate deep into the center of tumors.

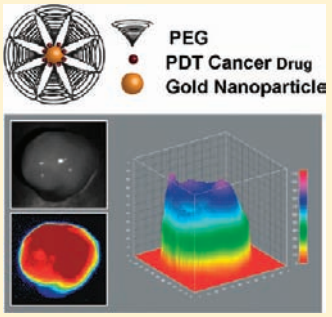

INTRODUCTION

Inefficient delivery and poor uptake of therapeutic drugs to solid tumors hamper the efficacy of cancer treatments.[1−3] Therefore, the "enhanced permeability and retention" (EPR) effect of solid tumors has been explored extensively as a target in the design of drug delivery systems.[4−7] Solid tumors behave differently from normal tissues, having several abnormalities, such as leaky blood vessels and a poor lymph system.[7−11] It is an important feature that nanosized particles can extravasate from the vasculature and passively accumulate in tumors.[5]

Inorganic nanoparticles, especially gold nanoparticles (Au NPs) with good biocompatibility, versatile surfaces, tunable sizes, and unique optical properties have received significant attention as drug delivery systems to improve targeting effect and efficacy for cancer treatments.[12−21] Covalent and noncovalent attachment are the two major approaches to deliver therapeutic drugs via Au NPs.[12,22−26] The covalent attachment approach requires not only structural modification of the therapeutic drugs, but also triggers to control the drug release, such as enzymes[25] and light[26]. Even though the modified pro-drugs can be stabilized by a chemical bond on the Au NP surface, the efficient release and efficacy of the drugs can be reduced. Although a significant number of available effective drugs have been modified to covalently bind to the Au NPs, noncovalent attachment maintaining the active drug structure without modification provides an attractive way to bind, deliver, and release the actual drug without needing such triggers. It allows the drug-loaded NPs to passively accumulate in the tumor and the noncovalently attached drug payload to be concentrated in the tumor mass.[12] Depending on the respective therapeutics and targets, the drug delivery approach must be chosen accordingly.

Photodynamic therapy (PDT) is a noninvasive treatment modality for cancers and other diseases.[27−30] Tumors and cancer cells can be eradicated by the combination of light, photosensitizer, and oxygen.[30−32] Previous studies have proven that hydrophobic PDT drugs can induce DNA and cell membrane damage to cancer cells via peroxidation of lipids, and further damage cellular organelles such as mitochondria through the formation of reactive oxygen species (ROS).[32−34] The majority of efficient photosensitizers are hydrophobic, which allows them to preferentially accumulate in the lipid bilayers of organelle membranes in cancer cells.[35] The hydrophobic nature of most photosensitizers makes them insoluble under physiological conditions and hinders their systemic administration.[35−37] Therefore, a relatively long time interval (∼1−3 days) between intravenous drug administration and therapeutic light irradiation is required to achieve the desirable drug concentration in a tumor for effective PDT treatment.[31] Moreover, PDT drugs can cause some side effects, such as prolonged skin photosensitivity, if allowed to stay in the body over long periods.[31] During the treatment intervals, patients must avoid daylight exposure. Therefore, a rapid and efficient delivery of the PDT drug to the target tumor and fast clearance would be ideal for PDT treatment.

A noncovalent delivery design that can solubilize and circulate the active drug payload systemically while providing an efficient and targeted release for subsequent treatment appears to be a preferable scenario for PDT.[12,38] Au NPs coated with polyethylene glycol (PEG) are promising drug delivery systems for the PDT of cancer.[12] The Au NP surface provides an amphiphilic

Received: September 30, 2010
Published: February 4, 2011

dx.doi.org/10.1021/ja108846h | J. Am. Chem. Soc. 2011, 133, 2583–2591

environment for lipophilic PDT drugs and can physically deactivate the drug until it is released from the NP.[12] The PEG on the Au NP surface provides solubility in water and minimizes any protein adsorption.[19] In addition, it has been widely reported that PEGylated NPs have a "stealth" character, which can postpone or prevent the rapid clearance by the reticular-endothelium system (RES).[39−41] Therefore, drugs on these Au NP carriers can have a prolonged circulation time in the blood.[41] Although Au NPs are not biodegradable, they have shown excellent biocompatibility and low toxicity.

The authors have previously evaluated the covalent and noncovalent PEGylated Au NP-based PDT drug delivery systems for HeLa cells.[42] In contrast to the slow intracellular release and reduced drug efficacy via the covalent attachment on Au NPs, noncovalent adsorption of the PDT drug to Au NPs showed efficient drug release into HeLa cancer cells by membrane-mediated diffusion without the need to use external stimuli.[42] It has been further demonstrated that the hydrophobic PDT drug silicon phthalocyanine 4 (Pc 4) noncovalently attached on PEGylated Au NPs is efficiently delivered to the tumor within minutes after intravenous injection. This is compared to the ∼48 h accumulation period needed for the free drug.[12,43−46] Successful PDT treatment can already be achieved 2 h after injection. The Au NP-delivered Pc 4 can cause tissue necrosis and shrinkage in tumor size following exposure to therapeutic light.[12]

Since the noncovalent delivery approach for hydrophobic therapeutic drugs, including PDT drugs,[12,22] via PEGylated Au NPs has attracted considerable attention, it is important to fully understand the *in vivo* drug delivery and release mechanism to the tumors for cancer therapy.

The aim of this work is to investigate the drug release mechanism in the tumor and to provide a correlation between the drug carrier (Au NP) and the drug itself *in vivo*. It has been reported that nanoparticles with a hydrodynamic diameter of less than 5.5 nm can be efficiently excreted via the renal clearance path.[47] We designed the Au NP core size with 5 nm diameter to remain small enough to be renally excreted while the hydrodynamic diameter of the PEGylated conjugate is 38 nm to improve stability, circulation time, and to achieve passive accumulation via the EPR effect. In addition, on a separate set of stability experiments of different PDT drug to Au NP ratios,[12] the drug loading was optimized to ∼30 PDT drug molecules per Au NP. This ratio was therefore also chosen for the animal studies presented here. The delivery, pharmacokinetics, and excretion dynamics of Au NPs and Pc 4 have been investigated with animal *in vivo* fluorescence imaging, elemental gold analysis, and histological imaging over a range of time points. We examine Au NP and Pc 4 localization in the tumor, providing support for the presented drug release mechanism and EPR effect in cancerous tissues (Figure 1) and for deep penetration of the drug into the interior of the tumor. This is a completely novel approach to deliver hydrophobic drugs fast and deep into tumors based on weak chemical interactions.

MATERIALS AND METHODS

Materials. The Au NPs were synthesized by the reduction of $HAuCl_4$ based on the modified Brust−Schiffrin method.[48,49] And the synthesized NPs were coated with mPEG-SH (MW 5000, Laysan Bio). The PDT drug silicon phthalocyanine 4 (Pc 4) was then mixed with the PEGylated Au NPs for 48 h and purified based on the procedure previously described.[12] The drug loading efficiency was optimized to 30 Pc 4 molecules per Au NP to obtain a stable conjugate in the aqueous phase. The final ratio of Pc 4 per Au NP in the PEGylated Au NP-Pc 4 conjugate was characterized by UV−vis spectroscopy. The average core size of Au NP was 5 nm in diameter, characterized by transmission electron microscopy (JEOL JEM-1200 EX electron microscope). The hydrodynamic diameter of the conjugates was 38.3 ± 0.4 nm, measured by dynamic light scattering (90Plus Particle Size Analyzer, Brookhaven Instruments Corporation). For intravenous injection, the administered conjugates in mice were based on a Pc 4 concentration of 1 mg kg^{-1}. An SPI-Mark silver enhancement kit was obtained from SPI Supplies Division of Structure Probe, Inc. (West Chester, PA) 1000 μg mL^{-1} gold standard solution in dilute hydrochloric acid was purchased from Inorganic Ventures. All other reagents were purchased from Sigma-Aldrich (St. Louis, MO) or Fisher Scientific (Pittsburgh, PA) and used as obtained.

Animal Experiments. Animal experiments were performed according to IACUC policies and guidelines of the Animal Care and Use Committee at Case Western Reserve University. Female athymic mice were obtained from the Athymic Animal Core Facility of the Cancer Research Center at Case Western Reserve University. Rat glioma (9 L) cancer cell lines overexpressing both EGFR and TfR were subcutaneously implanted in the flank of athymic mice (∼3 × 10^5 cells/implant). Tumors developed for 21 days prior to systemic injection with Au NP-Pc 4 conjugates. Animals were fed exclusively on a special rodent diet (Tekland 2018S; Harlan Laboratories, Inc.) to reduce autofluorescence performed under IACUC guidelines.

***In Vivo* Fluorescence Imaging.** Fluorescence *in vivo* imaging experiments were carried out at Case Western Reserve University in the Case Center for Imaging Research in Cleveland, Ohio. Mice with tumors (∼3−4 weeks after tumor implantation) were anaesthetized with isoflurane and injected intravenously via the tail with Au NP-Pc 4 at a dosage of Pc 4 at 1 mg kg^{-1} of total mouse body weight. Fluorescent multispectral images were obtained using the Maestro *In Vivo* Imaging System (Cambridge Research and Instrumentation, Inc., Woburn, MA). A Cy5 excitation filter (575−605 nm band-pass) and emission filter (645 nm long-pass) combination was used. Multispectral *in vivo* images were acquired under a constant exposure of 100 ms with a yellow filter acquisition setting of 630−850 nm in 2 nm increments. Multispectral images were unmixed into their component spectra (Pc 4, autofluorescence, and background) and these component images were used to gain quantitative information in terms of average fluorescence intensity by creating regions of interest (ROIs) around the tumors in the Pc 4 component images. Postanalysis spectral libraries were created by imaging a mouse pre- and post-injection to obtain a Pc 4 signal by subtraction of autofluorescence. Mice were imaged before injection (pre-injection), immediately following injection (10 min), every hour for 6 h (unless sacrificed at 4 h), and every 24 h until 7 days (unless sacrificed at 24 h). During the treatment period, mice were kept under normal ambient light cycles to mimic real-world drug applications.

Biodistribution Experiments. Blood from the Au NP conjugate-injected mice was collected in heparinized glass tubes and stored in the refrigerator at 4 °C until further processing. Tissues (tumor, heart, lung, spleen, liver, kidneys, urinary tract, large intestine, and stomach) from the mice were collected post mortem. The tissue samples were washed with normal saline, dried briefly with a paper towel and imaged with the same acquisition settings of *in vivo* fluorescence imaging 4 h, 24 h, or 7 days post-injection of the Au NP-Pc 4 conjugates. Multispectral images were unmixed into their component spectra (Pc 4, autofluorescence, and background) and Pc 4 component images were used to measure the Pc 4 intensity by creating ROIs associated with each organ. After imaging the collected tissues, they were weighed and stored in a −20 °C freezer until they could be analyzed for gold content via graphite furnace atomic absorption spectroscopy (GFAAS). Tissues, blood, urine, and feces collected from each mouse were then digested in Parr

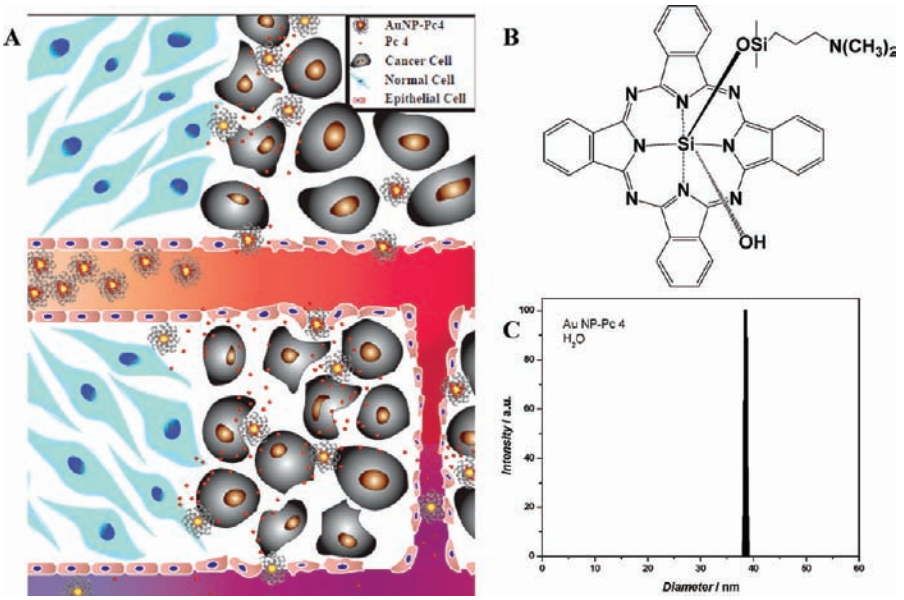

Figure 1. (A) Schematic of Au NP-Pc 4 conjugates circulation into the tumor. After circulating within the blood−vascular system, Au NP-Pc 4 extravasate through the endothelial cell layer of the blood vessels into cancerous tissues via the EPR effect. (B) Chemical structure of the PDT drug Pc 4. (C) The hydrodynamic diameter of the Au NP-Pc 4 conjugates measured by dynamic light scattering (DLS).

acid digestion vessels (Parr Instrument Company, Moline, IL) with 70% nitric acid at 120 °C for 2 h. Digested samples were diluted and analyzed by GFAAS in a GTA-110 with a programmable autosampler (Varian, Inc., Palo Alto, CA). The wavelength of the hollow cathode gold lamp was 242.8 nm and values for the concentration of gold in the samples were calibrated by a series of gold standard solutions.

Silver-Enhanced Staining of Excised Au NP-Pc 4 Injected Mice Organs. Tissue samples were fixed in 4% paraformaldehyde at room temperature for 24 h and embedded in a paraffin block. The tissue blocks were cut into 20-μm sections and placed on glass slides. The tissue slices were hydrated through a concentration series of ethanol (100%, 95%, 75%, and 50%) and placed in distilled water for 30 min. The silver enhancement reagents (developer and enhancer) were mixed immediately at a 1:1 ratio before the staining. The slides were gently tapped and the silver enhancement reagent mixture was placed on the slices for 15 min at room temperature. The staining was stopped by rinsing the slides with distilled water for 30 min. The tissue slides were then costained with hematoxylin and eosin (H&E). After washing, the slides were dehydrated in ethanol and cleared with xylene. The slides were finally mounted with Permount and cover glass. Stained sections were observed and images were obtained using a DM4000 B inverted microscope (Leica), and QCapture Pro imaging software (version 5.1.1.14; QImaging).

RESULTS AND DISCUSSION

Delivery of Pc 4 to the Tumor. As shown in Figure 1, the PDT drug Pc 4 can be stabilized via hydrophobic interaction to the Au NP surface. And the terminal amino group on the Pc 4 axial ligand can attach to the Au NP surface through N−Au interactions. Moreover, the PEG on the NPs provides a steric repulsion to stabilize the conjugates in the aqueous phase. Pc 4 on the Au NPs is protected from light by the Au NPs via excited state energy transfer to the NPs. The fluorescence of Pc 4 has been significantly quenched on Au NPs, as shown in Figure S1 of the Supporting Information. After the Au NP-Pc 4 conjugates are retained in the tumor, the drug release can be triggered by the hydrophobic attraction of the drug to the lipid membrane of the cancer cells.[42] The Pc 4 release from the conjugates will result in the increase of fluorescence intensity. In order to characterize the accumulation of Pc 4 delivered by the Au NPs *in vivo*, we accessed Pc 4 accumulation in tissues by monitoring the drug's fluorescence ($\lambda_{max,fl}$ = 680 nm) (Figures 2 and S2 of the Supporting Information), whereby the observed Pc 4 fluorescence reflects the concentration of the drug, which allowed analysis and optimization of the PDT treatment. Significant Pc 4 fluorescence was observed at the tumor area just minutes after intravenous tail vein injection of the Au NP-Pc 4 conjugates (Figure 2A). Drug accumulation in the tumor was quantified by identifying the tumor as a region of interest to measure its Pc 4 fluorescence intensity (Figure 2B). The average fluorescence intensity from Pc 4 acquired in the tumor areas quickly rose within 10 min post-injection and reached a plateau from 1 to 6 h post-injection (n = 5). A decrease in tumor fluorescence was observed 24 h post-injection. The rapid accumulation of drug within the tumor identifies a suitable treatment-time window for PDT. Au NP delivery of Pc 4 is a significant improvement in the time required by conventional means to achieve therapeutic doses in tumor tissue, reducing it from ~48 h (conventional) to ≤6 h (Au NPs).

Tumors derived from animals treated with the Au NP-Pc 4 were transected and imaged *ex vivo*. Pc 4 fluorescence was distributed throughout the whole tumor section with an intense fluorescence in the tumor's center after 4 h of Au NP-Pc 4 injection (Figure 2C,D). The two-dimensional fluorescence image of the harvested tumor at 4 h post-injection suggested Pc 4 distribution within the tumor and the corresponding surface plot of the fluorescence pixel intensities from the tumor region showed homogeneous Pc 4 distribution on the tumor surface (Figure 2C).

Ex vivo tumor fluorescence imaging further qualitatively verified that the best PDT treatment time must be within the first 6 h post-injection as the 4-h post-injection tumor showed the highest intensity compared to the 24-h tumor (Figure 2D). After 7 days, the fluorescence from the tumor nearly disappeared.

dx.doi.org/10.1021/ja108846h |*J. Am. Chem. Soc.* 2011, 133, 2583–2591

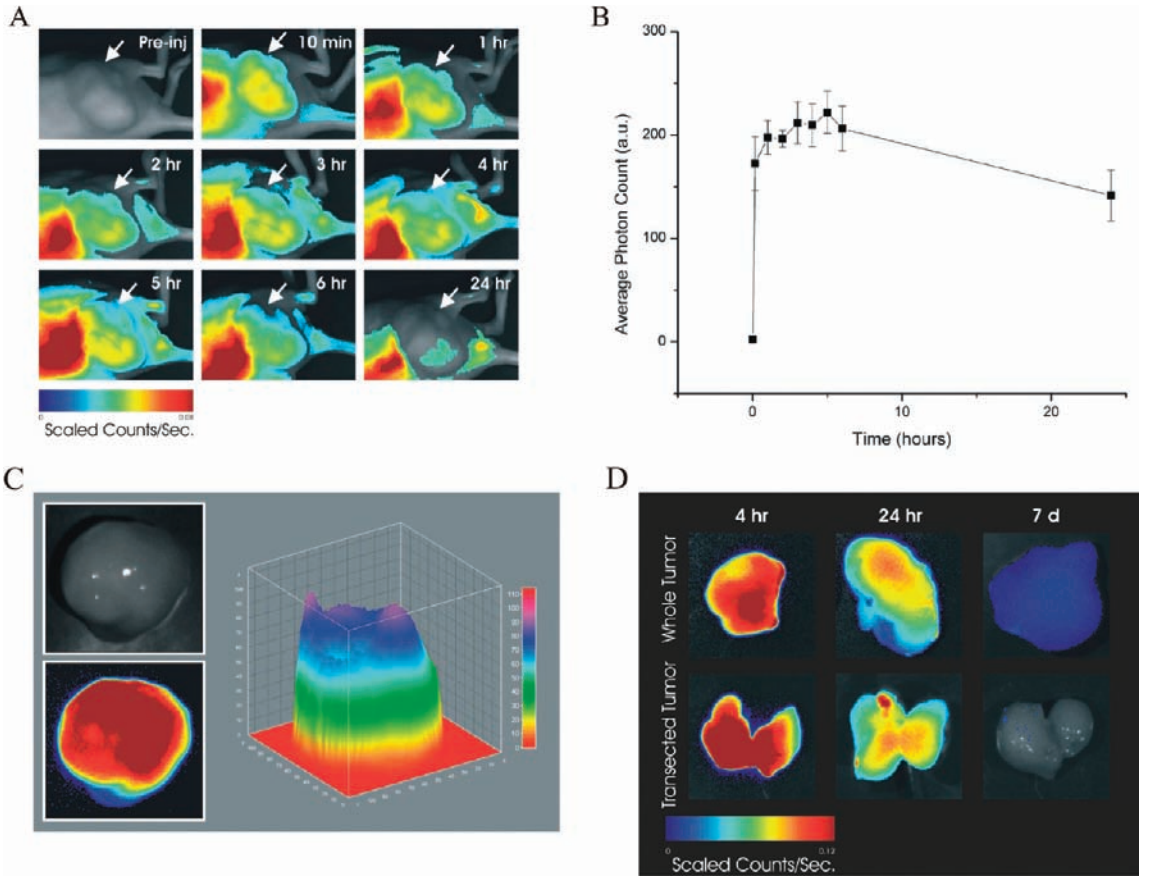

Figure 2. *In vivo* fluorescence imaging of Au NP-Pc 4 conjugates. Tumor bearing mice were injected intravenously with Au NP-Pc 4 conjugates at a Pc 4 dosage of 1 mg kg^{-1} mouse. (A) *In vivo* fluorescence imaging of a Au NP-Pc 4 conjugate injected mouse at various time points within 24 h. Arrows indicate tumor location. (B) The average fluorescence intensities from the tumor areas of 24-h post-injection mice ($n = 5$). (C) Picture of the tumor at 4 h post-injection (left) and the corresponding 3D surface plot (right) of pixel intensities (Pc 4 fluorescence) obtained from ImageJ. (D) Comparison of the fluorescence images in whole versus transected tumors at 4 h, 24 h and 7 days post-injection.

The intense Pc 4 fluorescence in the center of the tumor by 4 h (Figure 2D) showed very efficient diffusion of the PDT drug into the tumor. The drug biodistribution in the tumor tissue was further studied by examining the Pc 4 in the tumor cryosections. *Ex vivo* tumor cryosections were counterstained with DAPI to visualize cell nuclei (Figure 3A). Pc 4 accumulation was observed within the cytoplasm of the cells. Similar to the *ex vivo* tumor images, Pc 4 fluorescence tapered off dramatically by 7 days as shown in Figures 2D and 3A. The histological study of tumor tissues indicated the accumulation of Au NPs in the perivascular space at 4 h post-injection (Figure 3C). Au NPs in the tissue were enhanced by silver staining and visualized under microscopic magnification. The silver ions were reduced by hydroquinone to the elemental silver in presence of Au NP, which caused the growth of Au NPs.[41] In addition, more Au NPs were found in the center of the tumor area 24 h post-injection, which suggested permeation into the tumor. After 7 days, the Au NP concentration within tumor tissues dropped significantly.

It is hypothesized that the Au NPs with adsorbed Pc 4 release the drug by diffusion into hydrophobic areas within tissues (e.g., cellular membranes), but the Au NPs themselves do not enter the cells and undergo a different fate. In order to support our hypothesis, we carried out quantitative chemical analysis of tissue sections for gold and Pc 4. The concentration changes of both Au NP and Pc 4 (based on fluorescence) showed a similar trend during the 7-day post-injection period (Figure 4A). This implies that Pc 4 was indeed delivered to the tumor by the Au NPs after initial tail vein injection of the conjugates. At the 4 h post-injection time point, both Au NPs (% ID Au NP) and Pc 4 (fluorescence) showed the highest concentrations in the tumor of any time point measured. At 4 h post-injection, Au NPs were targeted to tumors with an average accumulation of 8 ± 6% ID presumably by the EPR effect. It was also found that 30 ±5.6% ID Au NPs remained in the blood at four hours after injection with a circulation half-life time of ~3 h (Figure 4B). This overlap in delivery and release dynamics supports the contention that the most suitable treatment time for PDT is within 6 h. This passive accumulation was shown to correlate with the blood clearance of Au NPs. The relatively long circulation of the NPs in the blood allowed significant accumulation of the drug in the tumor. Pc 4 drug release from the Au NP into the cells has a half-life of 2−3 h.[42] However, the significant drug release in the tumor at 10 min to 2 h after injections indicates that the drug release kinetics from the conjugates *in vivo* is different from that *in vitro*. The half-life of the drug release is decreased due to the more complex environment *in vivo*.

While Au NPs mainly localized in the perivascular space, Pc 4 in the tumor tissue showed a faster diffusion into the whole tumor at 4 h post-injection. When the Au NP-Pc 4 conjugates leak into the tumor through the endothelium of the blood vessels, the clearance of the conjugates is hampered by the lack of a

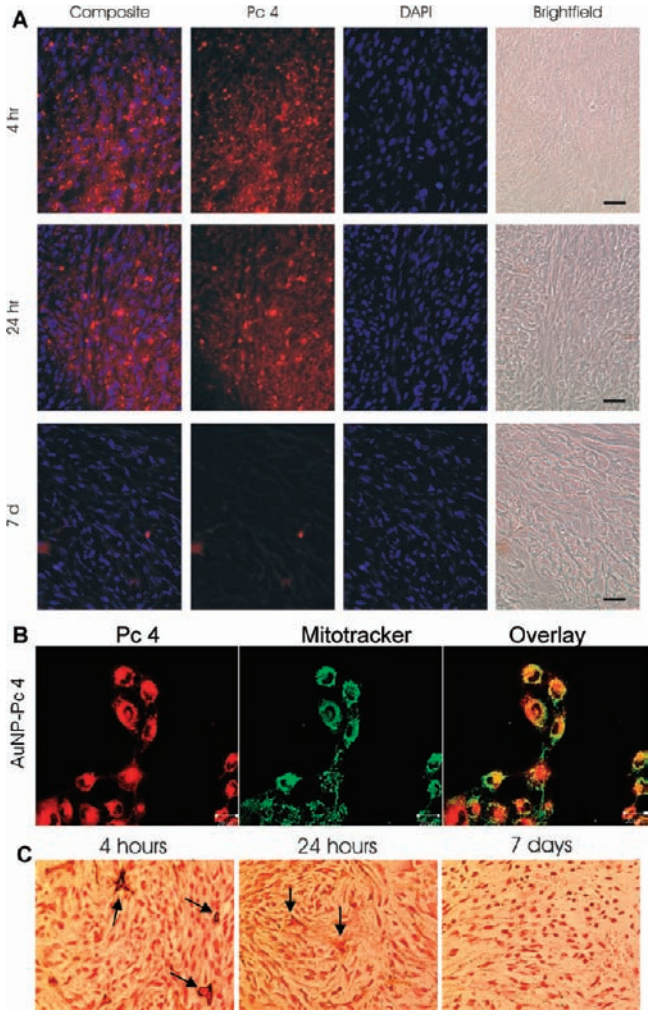

Figure 3. Au NP-Pc 4 accumulation in subcutaneous heterotopic tumors. (A) Cryosections of *ex vivo* tumors were counterstained with DAPI (blue) to visualize nuclei. Pc 4 fluorescence was captured using a standard Cy5 filter set (red). Images were overlaid to demonstrate Pc 4 uptake into the tumor. All images were captured at 40× magnification. Scale bar represents 100 μm. (B) Confocal images of the cancer cells incubated with Au NP-Pc 4 for 4 h stained with mitotracker green. (C) Au NPs visualized using silver enhancement staining in *ex vivo* paraffin-embedded tumor sections 4 h, 24 h, and 7 days post-injection. Arrows indicate the blood vasculatures. The size of Au NPs was enhanced by deposition of the elemental silver on the NP surface.

lymphatic recovery system.[7−10] This passive accumulation of the conjugates potentially results in the diffusion of the small drug molecules to the inner layers of the tumor by simple diffusion caused by a gradient of the drug concentration within the tumor. The noncovalent delivery approach and the inherent hydrophobic nature of Pc 4 are presumably the two major factors for the efficient release into the tumor cells. Our previous *in vitro* studies have shown that Pc 4 can be efficiently delivered by Au NPs into cancer cells within 4 h by membrane-mediated diffusion, while still remaining active for PDT.[42] In addition, these studies have also demonstrated that only a few Au NPs are taken up into the cells. While this noncovalent delivery approach has achieved efficient drug release *in vitro*, it promises a similarly efficient release into tumors in the animal model. On the basis of comparison with the dynamics of Au NPs, the faster diffusion of Pc 4 into the tumor (Figure 3 and 4) indicates that the drug is released from the NPs and transported via hydrophobic interaction with the plasma membranes and delivered into the cytoplasm of the tumor cells as described in Figure 1. We have further shown that the Au NP-delivered drug is mainly localized in mitochondria in the cells, similar to free Pc 4 (Figure 3B).[50] There is a driving force for Pc 4 into hydrophobic environments (Figure S3 of the Supporting Information). Low-density lipoproteins and other hydrophobic molecules in the bloodstream or tumors are in principle possible transport mechanisms.[51−54] However, the hydrodynamic diameter of the conjugates in serum did not change substantially as measured by DLS (Figure S4 of the Supporting Information). This shows that the PEGylation of the Au NPs effectively reduces the protein interactions with the drug and provides longer drug circulation time in the bloodstream.[3,5,55,56] The observed diffusional drug uptake into the cells is therefore due to the thermodynamic driving force toward their lipid membranes. After release from the Au NP, Pc 4 selectively enters the tumor cells by diffusion following the concentration gradient from areas of higher concentration to areas of lower concentration. A significant decrease of both the Au NPs and Pc 4 within 7 days in the tumors was also observed (Figure 3).

Biodistribution and Clearance of Pc 4. Six hours after injection of the conjugates, Pc 4 fluorescence intensity in the whole body leveled off and little fluorescence was observed 7 days post-injection (Figure S5A of the Supporting Information). The Pc 4 fluorescence from the tumor returned almost to baseline after 7 days (Figure S5B of the Supporting Information). It was also observed that the bladder area showed significant fluorescence after injection, suggesting that Pc 4 can be excreted in the form of urine by renal clearance in a very short time. Pc 4 fluorescence could be decreased over time by chemical quenching and structural change with enzymes produced in the organs (e.g., liver). Thus, the fluorescence intensity may not be a 100% exact tracking quantification method for *in vivo* studies, which is generally true for *in vivo* fluorescence workers.

On the basis of the fluorescence images, most of the Pc 4 drug molecules appear to be either excreted from the body or redistributed into other organs after a week of circulation within the body. Indeed, all of the organs as well as the tumor showed an overall decrease in Pc 4 fluorescence intensity within 7 days (Figure 5). The tumor at 4 h post-injection showed very high fluorescence intensities suggesting that the passive accumulation of Pc 4 by the NPs within the tumor was likely occurring. The liver, as part of the RES, also showed an accumulation of drug fluorescence. However, the spleen did not show much Pc 4 accumulation. Other organs such as the heart and lung showed moderate increases in Pc 4 fluorescence as well. At 4 h post-injection, the organs of excretion and digestion, including kidneys, urinary tract, large intestine, and stomach, all showed relatively intense Pc 4 fluorescence, while at 24 h and 7 days post-injection, the excretory organs showed less intense fluorescence. Meanwhile, the fluorescence from other organs decreased significantly within 7 days. Overall, the results suggest that Pc 4 was removed from both the cardio−pulmonary (heart, lung) and the immune systems and channeled into the excretory organs where Pc 4 could be finally removed from the body by renal clearance in the form of urine and by excretion in the form of feces.

Biodistribution and Clearance of Au NPs. A significant number of studies have been carried out to understand the

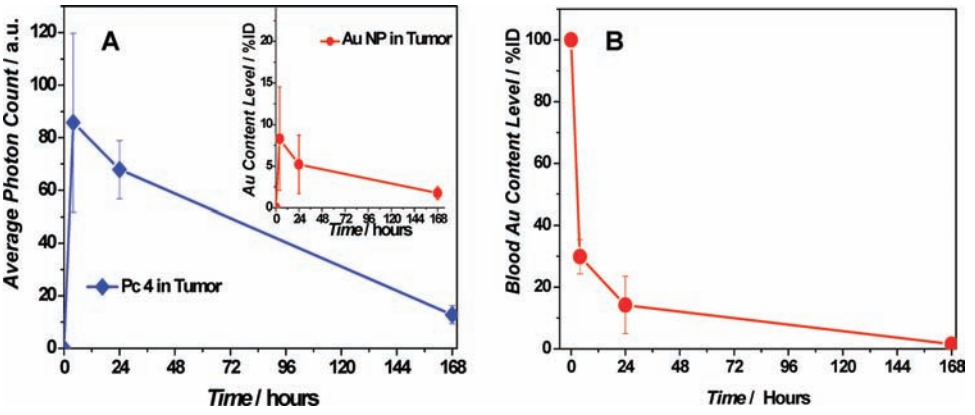

Figure 4. Au NP-Pc 4 accumulation in subcutaneous heterotopic tumors. (A) Graph of average Pc 4 fluorescence intensity; inset graph of Au concentration in tumors from the injected mice over a 7 day period ($n = 3$). (B) Gold concentration in blood based on total injected dose at different time points in Au NP-Pc 4 injected mice ($n = 5$).

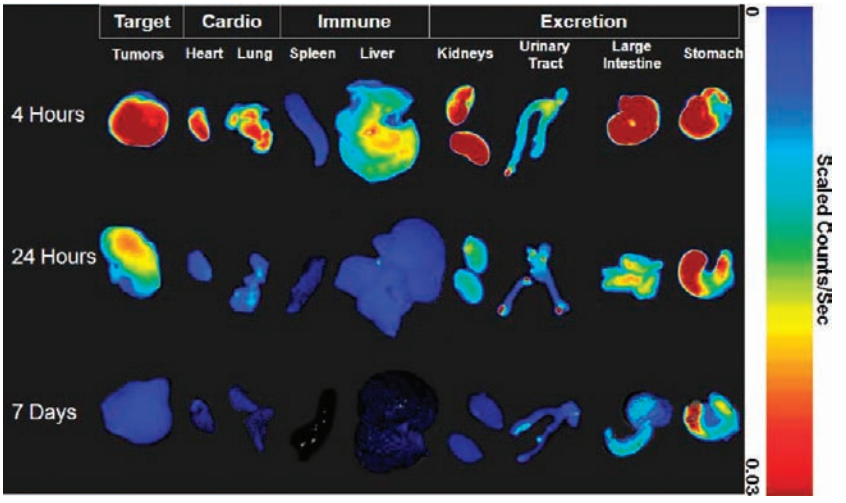

Figure 5. Biodistribution and elimination of Au NP-Pc 4 based on Pc 4 fluorescence. The Pc 4 fluorescence images of organs from the injected mice after dissection.

in vivo biodistribution of the Au NPs.[41,57−60] It is known that the biodistribution of Au NPs is very complex, which correlates with the surface ligands, charges, NP shapes and sizes. PEG-modified Au NPs have a long circulation time in the blood.[40,41] Fifty-four percent (54%) of injected Au NPs have been found in the blood at 0.5 h and the liver only showed the most NPs after 72 h.[40] Other studies found that the biodistribution of citrate-gold nanospheres are size-dependent and are mainly trapped by the liver 24 h after administration.[57,58] The 1.4 nm Au clusters ($Au_{55}(Ph_2PC_6H_4SO_3Na)_{12}Cl_6$) and 18 nm Au NPs have been studied in rats.[60] The 1.4 nm Au clusters showed some excretion by the kidneys and the hepatobiliary system 24 h after intravenous injection. And 47.5 ± 2.3% of the injected dose (ID) of 1.4 nm Au clusters was found in liver, while 18 nm Au NPs showed more than 90% of the ID in the liver with extremely low renal clearance.[60] However, little information about the fate of PEGylated Au NPs as a noncovalent drug carrier has been obtained in an animal model, since most studies have focused on short-term biodistribution (within 3 days). In this work, we investigated the Au NPs biodistribution up to 7 days after intravenous injection.

The Au NP-Pc 4 conjugates in this work have an average Au NP core size of 5 nm in diameter and can easily be quantified with GFAAS to determine biodistribution (Figures 6A and S6 of the Supporting Information). Blood, urine, feces, organs and tumors were collected at different time points after injection and analyzed for Au content. Most tissues including the tumor reached maximum gold accumulation by 4 h followed by a gradual decrease over time. A significant exception to this was observed in both the liver and spleen, where accumulation of the Au continued over time to reach a maximum at the latest time point measured, 7 days. Au NPs showed the highest concentration per gram of tissue in the spleen after 7 days post-injection (Figure 6A), while the liver showed the highest Au concentration in terms of % ID by accumulation of over 30% of the Au NPs (Figure S6 of the Supporting Information) after 7 days.

Au NPs were found in the kidneys and urinary tract over the next 7-day study. Urine samples from 4 h, 24 h, and 7 days showed the existence of the NPs, indicating that the Au NP-Pc 4 could be excreted by renal clearance. In addition, the Au NPs were found in feces samples from both 24-h and 7-day samples. In the tumor, heart, lung, kidney, and urinary track, the Au NP concentration significantly decreased after 7 days. Interestingly, the large intestine and stomach did not seem to exhibit a time-dependent increase or decrease in Au accumulation.

We found that PEGylated Au NPs circulating in the blood can be slowly opsonized and removed by the RES from the

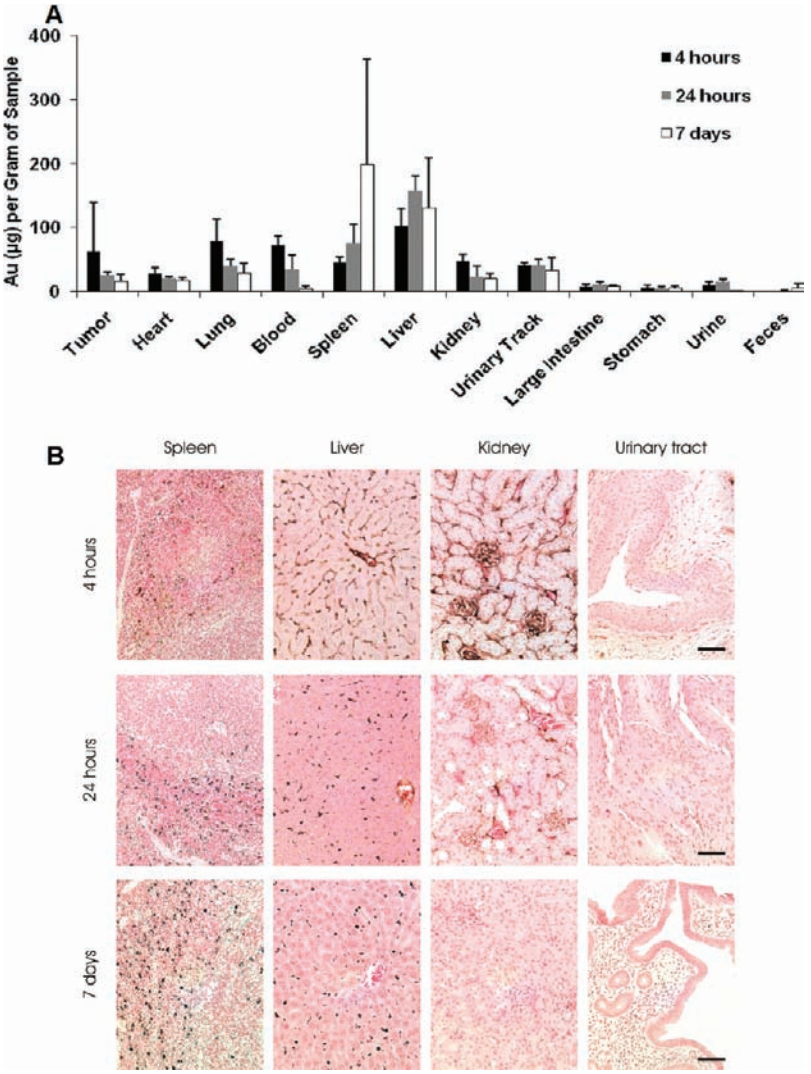

Figure 6. Assessment of Au NP-Pc 4 biodistribution on Au content. (A) Au (μg) per gram of sample in organs. Mice were injected with Au NP-Pc 4 ($n \geq 3$ per each time point). The total gold content in tissue samples was evaluated by GFAAS. (B) Histology studies of the organ tissues. Organ samples were removed from mice injected with Au NP-Pc 4 after 4 h, 24 h, and 7 days post-injection. The paraffin-embedded tissue slices were stained with hematoxylin, eosin, and silver enhancement reagents. The black and brownish spots indicate Au NPs in the tissues. Images were captured at 40× magnification. Scale bar represents 100 μm.

bloodstream, which is consistent with previous studies on nanomaterials such as polymeric NPs,[61] single-walled carbon nanotubes,[62] and quantum dots[63] (Figure 6B). Silver stained tissue samples showed significant accumulation of Au NPs in the liver and spleen (part of the RES) up to 7 days post-injection, which correlated well with the GFAAS analysis of the Au NPs in the organs (Figure 6). At 4 h post-injection, the NPs in the liver were mainly found in the blood vessels and liver sinusoids. After 24 h, the NPs were cleared from the blood vessels but remained in the liver sinusoids. A small number of Au NPs were observed in the hepatocytes in the liver. Histological examination suggested that macrophages in the spleen tissue were heavily loaded with the NPs (Figure 6B). Moreover, Au NPs were located in the glomerulus of the kidney, which supported the observation that the NPs could presumably be filtered by renal clearance in the form of urine. Over time, the number of Au NPs in the kidney decreased. A few Au NPs were found in the stroma of the urinary tract, further suggesting excretion of Au NPs through renal clearance.

Overall, PEGylated Au NPs, as the drug carriers circulating in the blood, can be slowly opsonized and removed from the bloodstream, followed by accumulation in the liver and spleen. When the NPs circulate in the body, the excretion process is rapid. Once the NPs are entrapped in the liver and spleen, this process slows down and depends on the digestion rate and metabolic activity of such cells as the Kupffer cells and macrophages. A significant number of Au NPs was found in the urine and feces sampled within 7 days. Therefore, the kidneys and urinary tract are important excretion organs for Au NPs. In addition, part of the Au NPs can be excreted by the hepatobiliary system (such as stomach and large intestine).

Correlation Between Distributions of Au NPs and Pc 4 *in Vivo*. This work also demonstrates the consequences of noncovalent drug delivery, which result in efficient drug delivery into the tumor cells and simultaneously in a minimal uptake of the NPs into the cells. On the basis of the mechanisms and driving forces described above, the drug separates from the Au NP carrier while it is retained in the tumor tissue and taken up into the

dx.doi.org/10.1021/ja108846h |*J. Am. Chem. Soc.* 2011, 133, 2583–2591

tumor cells by membrane-mediated diffusion. The PEG coated Au NPs do not necessarily need to enter into the cancer cells to deliver drugs. After the drug is deposited into the cells, the NPs keep circulating in the body and have their own biodistribution. Eventually, both the NP and the Pc 4 have different distribution profiles upon injection of the Au NP-Pc 4 conjugates into the mice. In the tumor site, the EPR effect was the driving force to accumulate the conjugates into the tumor area where they could interact with tumor tissue and deliver drugs, as indicated in the accumulation of both entities in the tumor at 4 h post injection (Figures 5 and 6A). While the drug localizes predominately in the tumor, the NPs have been filtered by the liver and spleen. Consequently, there is not a strict correlation between Au NP and Pc 4 concentrations in tissues such as liver and spleen. We have already successfully treated tumors in mice via PDT. We will publish the outcome of these experiments, focusing on their biomedical nature, separately.

CONCLUSIONS

In this work, the drug delivery mechanism and pharmacokinetics of noncovalent Au NP-Pc 4 conjugates were studied over a period of 7 days. No adverse effects of the conjugates were observed in the mice in this study. A PDT treatment time window from 1 to 6 h after intravenous administration has been determined. A correlation of the drug and Au NPs in the tumor was examined. The noncovalent delivery approach provided surprisingly efficient release and penetration of the drug into the tumor. This is a novel approach to deliver not only PDT drugs, but also other hydrophobic drugs rapidly and deep into tumors. Over the 7 day study period, fast drug excretion has been observed by *in vivo* and *ex vivo* fluorescence imaging. Although Au NPs have an overall longer retention time, especially in liver and spleen, their excretion pathways have been identified. Both the drug and the Au NPs were found to be excreted from the body by renal clearance and the hepatobiliary system. This work demonstrates efficient noncovalent drug delivery by PEGylated gold NPs on the example of Pc 4, but may have ramifications for a much wider range of hydrophobic drugs.

ASSOCIATED CONTENT

Supporting Information. Fluorescence of Pc 4 (Figures S1−S6). This material is available free of charge via the Internet at http://pubs.acs.org.

AUTHOR INFORMATION

Corresponding Author

axb110@case.edu;
jxb206@case.edu;
burda@case.edu

Author Contributions

[§]These authors contributed equally.

ACKNOWLEDGMENT

We thank Prof. Hisashi Fujioka for helpful discussions and Dr. James Faulk for assistance in gold GFAAS analysis. This work was financially supported by the BRTT Center for Targeted Nanoparticles for Imaging and Therapeutics at Case Western Reserve University (to C.B.). This work was also supported by an ongoing center grant from the National Foundation for Cancer Research (to J.P.B.) and a fellowship award (to A.M.B.). In addition, the project described was supported by Grant No. K01EB006910 (to A.M.B.) from the National Institute of Biomedical Imaging and Bioengineering. The content is solely the responsibility of the authors and does not necessarily represent the official views of the National Institute of Biomedical Imaging and Bioengineering or the National Institutes of Health.

REFERENCES

(1) Heldin, C. H.; Rubin, K.; Pietras, K.; Ostman, A. *Nat. Rev. Cancer* **2004**, *4*, 806.
(2) Sugahara, K. N.; Teesalu, T.; Karmali, P. P.; Kotamraju, V. R.; Agemy, L.; Girard, O. M.; Hanahan, D.; Mattrey, R. F.; Ruoslahti, E. *Cancer Cell* **2009**, *16*, 510.
(3) Langer, R. *Nature* **1998**, *392*, 5.
(4) Torchilin, V. P. *Adv. Drug Delivery Rev.* **2006**, *58*, 1532.
(5) Peer, D.; Karp, J. M.; Hong, S.; Farokhzad, O. C.; Margalit, R.; Langer, R. *Nat. Nanotechnol.* **2007**, *2*, 751.
(6) Cho, K. J.; Wang, X.; Nie, S. M.; Chen, Z.; Shin, D. M. *Clin. Cancer Res.* **2008**, *14*, 1310.
(7) Maeda, H. *Adv. Enzyme Regul.* **2001**, *41*, 189.
(8) Matsumura, Y.; Maeda, H. *Cancer Res.* **1986**, *46*, 6387.
(9) Baban, D. F.; Seymour, L. W. *Adv. Drug Delivery Rev.* **1998**, *34*, 109.
(10) Iyer, A. K.; Khaled, G.; Fang, J.; Maeda, H. *Drug Discov. Today* **2006**, *11*, 812.
(11) Allen, T. M.; Cullis, P. R. *Science* **2004**, *303*, 1818.
(12) Cheng, Y.; Samia, A. C.; Meyers, J. D.; Panagopoulos, I.; Fei, B. W.; Burda, C. *J. Am. Chem. Soc.* **2008**, *130*, 10643.
(13) Elbakry, A.; Zaky, A.; Liebl, R.; Rachel, R.; Goepferich, A.; Breunig, M. *Nano Lett.* **2009**, *9*, 2059.
(14) Jain, P. K.; Huang, X.; El-Sayed, I. H.; El-Sayed, M. *Acc. Chem. Res.* **2008**, *41*, 1578.
(15) Gao, J.; Gu, H.; Xu, B. *Acc. Chem. Res.* **2009**, *42*, 1097.
(16) Ghosh, P.; Han, G.; De, M.; Kim, C. K.; Rotello, V. M. *Adv. Drug Delivery Rev.* **2008**, *60*, 1307.
(17) Chatterjee, D. K.; Fong, L. S.; Zhang, Y. *Adv. Drug Delivery Rev.* **2008**, *60*, 1627.
(18) Paciotti, G. F.; Myer, L.; Weinreich, D.; Goia, D.; Pavel, N.; McLaughlin, R. E.; Tamarkin, L. *Drug Deliv.* **2004**, *11*, 169.
(19) Paciotti, G. F.; Kingston, D. G. I.; Tamarkin, L. *Drug Dev. Res.* **2006**, *67*, 47.
(20) Boisselier, E.; Astruc, D. *Chem. Soc. Rev.* **2009**, *38*, 1759.
(21) Hone, D. C.; Walker, P. I.; Evans-Gowing, R.; FitzGerald, S.; Beeby, A.; Chambrier, I.; Cook, M. J.; Russell, D. A. *Langmuir* **2002**, *18*, 2985.
(22) Kim, C. K.; Ghosh, P.; Pagliuca, C.; Zhu, Z.; Menichetti, S.; Rotello, V. M. *J. Am. Chem. Soc.* **2009**, *131*, 1360.
(23) Hong, R.; Han, G.; Fernandez, J. M.; Kim, B. J.; Forbes, N. S.; Rotello, V. M. *J. Am. Chem. Soc.* **2006**, *128*, 1078.
(24) Gibson, J. D.; Khanal, B. P.; Zubarev, E. R. *J. Am. Chem. Soc.* **2007**, *129*, 11653.
(25) Hwu, J. R.; Lin, Y. S.; Josephrajan, T.; Hsu, M.; Cheng, F.; Yeh, C.; Su, W.; Shieh, D. *J. Am. Chem. Soc.* **2009**, *131*, 66.
(26) Agasti, S. S.; Chompoosor, A.; You, C.; Ghosh, P.; Kim, C. K.; Rotello, V. M. *J. Am. Chem. Soc.* **2009**, *131*, 5728.
(27) Dougherty, T. J.; Grinday, G. B.; Fiel, R.; Weishaupt, K. R.; Boyle, D. G. *J. Natl. Cancer Inst.* **1975**, *55*, 115.
(28) Dougherty, T. J. *Crit. Rev. Oncol. Hemat.* **1984**, *2*, 83.
(29) Dougherty, T. J.; Gomer, C. J.; Henderson, B. W.; Jori, G.; Kessel, D.; Korbelik, M.; Moan, J.; Peng, Q. *J. Natl. Cancer Inst.* **1998**, *90*, 889.
(30) Castano, A. P.; Mroz, P.; Hamblin, M. R. *Nat. Rev. Cancer* **2006**, *6*, 535.

(31) Dolmans, D. E. J. G. J.; Fukumura, D.; Jain, R. K. *Nature Rev.* **2003**, *3*, 380.
(32) Oleinick, N. L.; Morris, R. L.; Belichenko, T. *Photochem. Photobiol. Sci.* **2002**, *1*, 1.
(33) Girotti, A. W. *J. Photochem. Photobiol. B: Biol.* **2001**, *63*, 103.
(34) Hong, I. S.; Greenberg, M. M. *J. Am. Chem. Soc.* **2005**, *127*, 10510.
(35) Konan, Y. N.; Gurny, R.; Allemann, E. *J. Photochem. Photobiol. B:Biol.* **2002**, *66*, 89.
(36) van Nostrum, C. F. *Adv. Drug Delivery Rev.* **2004**, *56*, 5.
(37) Kessel, D. *Adv. Drug Delivery Rev.* **2004**, *56*, 7.
(38) Roy, I.; Ohulchanskyy, T. Y.; Pudavar, H. E.; Bergey, E. J.; Oseroff, A. R.; Morgan., J.; Dougherty, T. J.; Prasad, P. N. *J. Am. Chem. Soc.* **2003**, *125*, 7860.
(39) Gref, R.; Lück, M.; Quellec, P.; Marchand, M.; Dellacherie, E.; Harnisch, S.; Blunk, T.; Müller, R. H. *Colloids Surf. B: Biointerfaces* **2000**, *18*, 301.
(40) Niidome, T.; Yamagata, M.; Okamoto, Y.; Akiyama, Y.; Takahashi, H.; Kawano, T.; Katayama, Y.; Niidome, Y. *J. Controlled Release* **2006**, *114*, 343.
(41) Perrault, S. D.; Walkey, C.; Jennings, T.; Fischer, H. C.; Chan, W. C. W. *Nano Lett.* **2009**, *9*, 1909.
(42) Cheng, Y.; Samia, A. C.; Li, J.; Kenney, M. E.; Resnick, A.; Burda, C. *Langmuir* **2010**, *26*, 2248.
(43) Oleinick, N. L.; Antunez, A. R.; Clay, M. E.; Rihter, B. D.; Kenney, M. E. *Photochem. Photobiol.* **1993**, *57*, 242.
(44) Miller, J. D.; Baron, E. D.; Scull, H.; Hsia, A.; Berlin, J. C.; McCormick, T.; Colussi, V.; Kenney, M. E.; Cooper, K. D.; Oleinick, N. L. *Toxicol. Appl. Pharmacol.* **2007**, *224*, 290.
(45) Bai, L.; Guo, J.; Bontempo, F. A., III; Eiseman, J. L. *Photochem. Photobiol.* **2009**, *85*, 1011.
(46) Colussi, V. C.; Feyes, D. K.; Mulvihill, J. W.; Li, Y. S.; Kenney, M. E.; Elmets, C. A.; Oleinick, N. L.; Mukhtar, H. *Photochem. Photobiol.* **1999**, *69*, 236.
(47) Choi, H. S.; Liu, W.; Misra, P.; Tanaka, E.; Zimmer, J. P.; Ipe, B. I.; Bawendi, M. G.; Frangioni, J. V. *Nat. Biotechnol.* **2007**, *25*, 1165.
(48) Duan, H.; Nie, S. *J. Am. Chem. Soc.* **2007**, *129*, 2412.
(49) Brust, M.; Walker, M.; Bethell, D.; Schiffrin, D. J.; Whyman, R. *J. Chem. Soc., Chem. Comm.* **1994**, *7*, 801.
(50) Morris, R. L.; Azizuddin, K.; Lam, M.; Berlin, J.; Nieminen, A. L.; Kenney, M. E.; Samia, A. C. S.; Burda, C.; Oleinick, N. L. *Cancer Res.* **2003**, *63*, 5194.
(51) Kongshaug, M.; Moan, J.; Brown, S. B. *Br. J. Cancer* **1989**, *59*, 184.
(52) Maziere, J. C.; Morliere, P.; Santus, R. *J. Photochem. Photobiol. B: Biol.* **1991**, *8*, 351.
(53) Haylett, A. K.; Moore, J. V. *J. Photochem. Photobiol. B: Biol.* **2002**, *66*, 171.
(54) Polo, L.; Valduga, G.; Jori, G.; Reddi, E. *Int. J. Biochem. Cell Biol.* **2002**, *34*, 10.
(55) Torchilin, V. P. *J. Controlled Release* **2001**, *73*, 137.
(56) Zhang, L.; Chan, J. M.; Gu, F. X.; Rhee, J.-W.; Wang, A. Z.; Radovic-Moreno, A. F.; Alexis, F; Langer, R.; Farokhzad, Omid C. *ACS Nano* **2008**, *2*, 1696.
(57) Sonavane, G.; Tomod, K.; Makin, K. *Colloids Surf. B: Biointerfaces* **2008**, *66*, 274.
(58) Sadauskas, E.; Wallin, H.; Stoltenberg, M.; Vogel, U.; Doering, P.; Larsen, A.; Danscher, G. *Particle Fibre Toxicol.* **2007**, *4*, 10.
(59) Lipka, J.; Semmler-Behnke, Manuela; Sperling, R, A.; Wenk, A.; Takenaka, S.; Schleh, C.; Kissel, T.; Parak, W. J.; Kreyling, W. G. *Biomaterials* **2010**, *31*, 6574.
(60) Semmler-Behnke, M.; Kreyling, W. G.; Lipka, J.; Fertsch, S.; Wenk, A.; Takenaka, S.; Schmid, G.; Brandau, W. *Small* **2008**, *4*, 2108.
(61) Moghimi, S. M.; Hunter, A. C.; Murray, J. C. *Pharmacol. Rev.* **2001**, *53*, 283.
(62) Liu, Z.; Cai, W.; He, L.; Nakayama, N.; Chen, K.; Sun, X.; Chen, X.; Dai, H. *Nat. Nanotechnol.* **2006**, *2*, 47.
(63) Choi, H. S.; Ipe, B. I.; Misra, P.; Lee, J. H.; Bawendi, M. G.; Frangioni, J. V. *Nano Lett.* **2009**, *9*, 2354.